MOLECULAR IMAGING AND BIOLOGY

Mol Imaging Biol (2020) 22:1151–1160
DOI: 10.1007/s11307-020-01517-5

Published Online: 20 July 2020

WMIS World Molecular Imaging Society
esmi European Society for Molecular Imaging

Check for updates

RESEARCH ARTICLE

Synthesis and Characterization of 9-(4-[^{18}F]Fluoro-3-(hydroxymethyl)butyl)-2-(phenylthio)-6-oxopurine as a Novel PET Agent for *Mutant* Herpes Simplex Virus Type 1 Thymidine Kinase Reporter Gene Imaging

Takeshi Fuchigami,[1,2] Tom Haywood,[2] Gayatri Gowrishankar,[2] David Anders,[2] Mohammad Namavari,[2] Mirwais Wardak,[2] Sanjiv Sam Gambhir[2,3]

[1]*Department of Hygienic Chemistry, Graduate School of Biomedical Sciences, Nagasaki University, 1-14 Bunkyo-machi Nagasaki 852-8521 Japan*

[2]*Department of Radiology, Molecular Imaging Program at Stanford (MIPS), Stanford University School of Medicine, 318 Campus Drive, Room E150A Stanford CA 94305 USA*

[3]*Department of Bioengineering and Materials Science & Engineering, Bio-X Program, Stanford University, 318 Campus Dr., Room E150 Stanford Stanford CA 94305 USA*

Abstract

Purpose: [^{18}F]FHBG has been used as a positron emission tomography (PET) imaging tracer for the monitoring of herpes simplex virus type 1 thymidine kinase (HSV1-tk), a reporter gene for cell and gene therapy in humans. However, this tracer shows inadequate blood-brain barrier (BBB) penetration and, therefore, would be limited for accurate quantification of reporter gene expression in the brain. Here, we report the synthesis and evaluation of 9-(4-[^{18}F]fluoro-3-(hydroxymethyl)butyl)-2(phenylthio)-6-oxopurine ([^{18}F]FHBT) as a new PET tracer for imaging reporter gene expression of HSV1-tk and its mutant HSV1-sr39tk, with the aim of improved BBB penetration.

Procedures: [^{18}F]FHBT was prepared by using a tosylate precursor and [^{18}F]KF. The cellular uptake of [^{18}F]FHBT was performed in HSV1-sr39tk-positive (+) or HSV1-sr39tk-negative (–) MDA-MB-231 breast cancer cells. The specificity of [^{18}F]FHBT to assess HSV1-sr39tk expression was evaluated by *in vitro* blocking studies using 1 mM of ganciclovir (GCV). Penetration of [^{18}F]FHBT and [^{18}F]FHBG across the BBB was assessed by dynamic PET imaging studies in normal mice.

Results: The tosylate precursor reacted with [^{18}F]KF using Kryptofix2.2.2 followed by deprotection to give [^{18}F]FHBT in 10 % radiochemical yield (decay-corrected). The uptake of [^{18}F]FHBT in HSV1-sr39tk (+) cells was significantly higher than that of HSV1-sr39tk (–) cells. In the presence of GCV (1 mM), the uptake of [^{18}F]FHBT was significantly decreased, indicating that [^{18}F]FHBT serves as a selective substrate of HSV1-sr39TK. PET images and time-activity

Electronic supplementary material The online version of this article (https://doi.org/10.1007/s11307-020-01517-5) contains supplementary material, which is available to authorized users.

Correspondence to: Sanjiv Gambhir; *e-mail:* sgambhir@stanford.edu

curves of [18F]FHBT in the brain regions showed similar initial brain uptakes (~ 12.75 min) as [18F]FHBG ($P > 0.855$). Slower washout of [18F]FHBT was observed at the later time points (17.75 – 57.75 min, $P > 0.207$).

Conclusions: Although [18F]FHBT showed no statistically significant improvement of BBB permeability compared with [18F]FHBG, we have demonstrated that the 2-(phenylthio)-6-oxopurine backbone can serve as a novel scaffold for developing HSV1-tk/HSV1-sr39tk reporter gene imaging agents for additional research in the future.

Key words: Positron emission tomography, Reporter gene imaging, HSV1-tk, [18F]FHBT, Radiochemistry, Blood-brain barrier

Introduction

Reporter gene-based molecular imaging, including positron emission tomography (PET) with the appropriate reporter probes, is a noninvasive and quantitative imaging tool for monitoring specific biological process, investigating protein-protein interactions, tracking the fate of transplanted cells, and assessing cell-based therapeutic gene delivery efficiency and treatment efficacy. There is a growing importance of monitoring gene therapy in the central nervous system (CNS). However, a noninvasive clinical evaluation method for gene therapies in CNS diseases has not yet been established [1]. Recently, we demonstrated the utility of pyruvate kinase M2 and its corresponding radiotracer [18F]DASA-23 as a potential PET reporter gene/reporter probe system for use in the CNS [2]. However, further detailed research may be needed to proceed this system for clinical practice. The genes encoding herpes simplex virus type 1 thymidine kinase (HSV1-tk) and the *mutant* version such as HSV1-sr39tk are the most widely used PET reporter system in preclinical studies and clinical studies [3–5]. Specific PET reporter probes are phosphorylated by HSV1-TK upon internalization into the HSV1-TK-expressing cells resulting in metabolic capture and retention. Therefore, this system can indirectly infer the location, degree of expression, and duration of the gene of interest [6]. The current PET radiotracers for imaging of HSV1-tk and its mutant include pyrimidine analogs such as 2′-deoxy-2′-[18F]-fluoro-1-beta-D-arabinofuranosyl-5-iodouracil ([18F]FIAU) [7] and 2′-deoxy-2′-[18F]-fluoro-5-ethyl-1-β-D-arabinofuranosyl-uracil ([18F]FEAU) [8] or purine-based nucleosides such as 9-((3-[18F]fluoro-1-hydroxy-2-propoxy)-methyl)guanine ([18F]FHPG) [9] and 9-[4-[18F]fluoro-3-(hydroxymethyl) butyl]guanine ([18F]FHBG) [10] (Fig. 1a). Among them, only [18F]FHBG has been used as a PET imaging agent for the monitoring of HSV1-tk in gene and cell therapies in human [11–13]. Peñuelas et al. reported clinical PET studies of [18F]FHBG to monitor HSV1-tk gene expression after intratumoral injection in hepatocellular carcinoma patients [11]. Recently, Keu et al. demonstrated that PET imaging with [18F]FHBG can track HSV1-tk (+) chimeric antigen receptor T cells in patients with high-grade glioma [13]. Mutant HSV1-TK enzymes such as HSV1-sr39TK have been developed to utilize acyclovir derivatives for more effective suicide gene therapy [14]. [18F]FHBG has minimum affinity for mammalian TK enzymes, and a high affinity for the HSV1-sr39TK enzyme when compared with HSV1-TK [15]. Highly sensitive PET imaging of reporter gene expression has been achieved in HSV1-sr39 (+) tumor-bearing mice [15]. Unfortunately, [18F]FHBG has shown inadequate BBB permeability, greatly limiting its ability to quantify cerebral reporter gene expression, such as stem cells and therapeutic T cells administered in the brain for treatment of neurodegenerative disorders and glioblastoma. Martinez-Quintanilla et al. reported that PET imaging with [18F]FHBG allowed to detect intracranially implanted mesenchymal stem cells engineered to co-express HSV1-TK in mice brain [16]. However, low penetration of [18F]FHBG through the BBB can complicate longitudinal quantitative monitoring of the expression of stem cells transplanted to patients with brain disorders. Salabert et al. demonstrated that PET uptake of [18F]FHBG correlated well with the number of grafted Neuro2A cells stably expressing HSV-1 TK in a brain injury rodent model. However, the tracer was injected intracerebrally instead of intravenously [17]. To overcome this limitation, there is a great need to develop PET agents which are capable of crossing the intact BBB for imaging the expression of HSV1-tk and its mutants in the brain. It is reported that successful radioligands or drugs for CNS applications have log P values in the range 1.5–2.5 and a molecular weight < 400 Da [18, 19]. Accordingly, low lipophilicity of [18F]FHBG (Clog$P = -1.41$, calculated by Chem BioDraw Ultra 13.0) is considered to limit its BBB penetration. Several 6-oxopurine derivatives showed potent inhibitory activity against HSV1-tk [20]. Among them, 9-(4-hydroxybutyl)-2-phenylthio-6-oxopurine (HBT), which possesses a moderate calculated log$P$ (Clog$P$) value of 1.98, inhibited the recombinant HSV1-TK with IC_{50} values of 0.5 μM. We hypothesized that this lipophilic compound could be used as a scaffold for developing new PET agents that can freely cross the BBB. In this study, we designed a new PET agent, 9-(4-[18F]fluoro-3-(hydroxymethyl)butyl)-2(phenylthio)-6-oxopurine ([18F]FHBT), which combined parts of FHBG and HBT (Fig. 1b). FHBT has preferable physiochemical properties (MW = 348.40 Da, Clog$P = 1.94$) and a 9-(3-

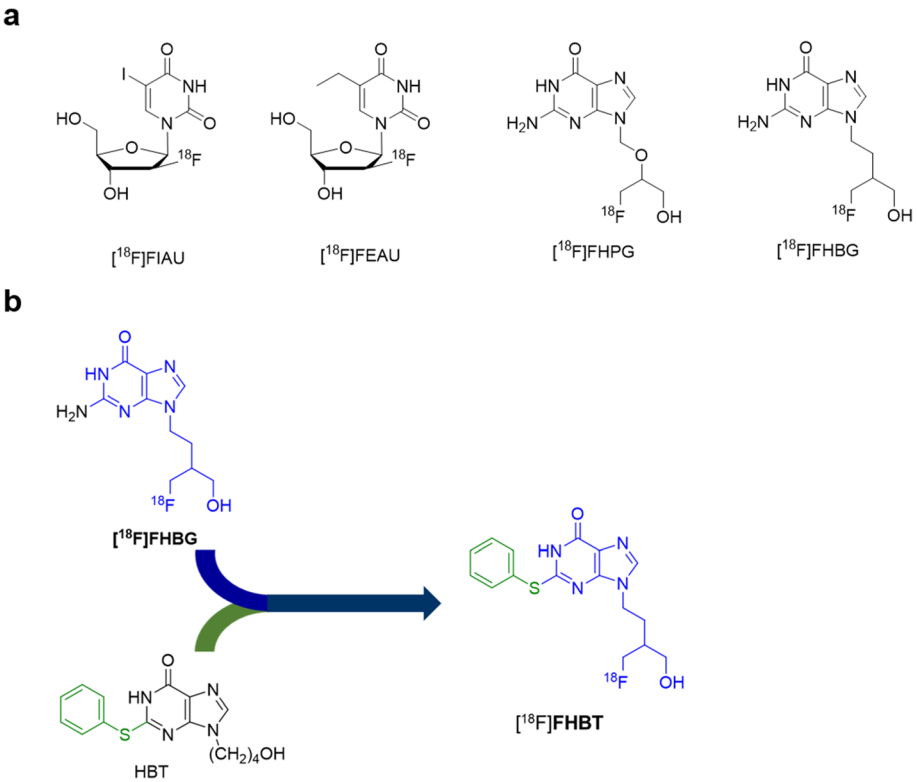

Fig. 1 **a** Chemical structures of 2′-deoxy-2′-[^{18}F]-fluoro-1-beta-D-arabinofuranosyl-5-iodouracil ([^{18}F]FIAU), 2′-deoxy-2′-[^{18}F]-fluoro-5-ethyl-1-β-D-arabinofuranosyl-uracil ([^{18}F]FEAU), 9-((3-[^{18}F]fluoro-1-hydroxy-2-propoxy)-methyl)guanine ([^{18}F]FHPG), and 9-[4-[^{18}F]fluoro-3-(hydroxymethyl)butyl]guanine ([^{18}F]FHBG). **b** Design of 9-(4-fluoro-3-(hydroxymethyl)butyl)-2(phenylthio)-6-oxopurine ([^{18}F]FHBT) derived from moieties of [^{18}F]FHBG and 9-(4-hydroxybutyl)-2-phenylthio-6-oxopurine (HBT) as a new PET radiotracer for imaging reporter gene expression of HSV1-tk and its mutant variants.

hydroxymethylbutyl) group within the molecule as in FHBG and FHPG. We postulated that FHBT may pass through the BBB freely and undergo phosphorylation by HSV1-TK and its mutants, resulting in specific trapping in HSV1-tk (wild type and mutants) expressing cells in the CNS. We herein report the synthesis of [^{18}F]FHBT and its preliminary biological evaluation as a novel PET agent for imaging of HSV1-tk expression in the brain.

Materials and Methods

General

All commercial reagents and solvents were purchased from Thermo Fisher Scientific (Waltham, MA), Sigma–Aldrich (St. Louis, MO) and Merck (Darmstadt, Germany). The regents and solvents were used without further purification unless otherwise specified. No-carrier-added [^{18}F]fluoride was prepared by the ^{18}O(p, n)^{18}F nuclear reaction on a GE PETtrace cyclotron. [^{18}F]Fluoride processing and radiosynthesis of [^{18}F]FHBT were performed in the GE TRACERlab FX-FN synthesis module (GE Medical System, Milwaukee, WI). Purification of [^{18}F]FHBT was performed on a Dionex HPLC system (Dionex Corporation, Sunnyvale, CA) equipped with a Dionex P680 quaternary gradient pump, a Knauer K-2001 UV detector (Berlin, Germany) set at 254 nm and a radioactivity detector (Carroll & Ramsey Associates, model 105S, Berkeley, CA). Radioactivity measurements were performed by a CRC-15R PET dose calibrator (Capintec Inc., Ramsey, NJ). Electron spray ionization mass spectrometry was carried out by the Vincent Coates Foundation Mass Spectrometry Laboratory, Stanford University. ^{1}H and ^{13}C nuclear magnetic resonance (NMR) spectra were taken on an Agilent 400 MHz spectrometer.

Synthesis of FHBT

Synthetic methods and analytical data for non-radioactive FHBT are available in the Electronic Supplementary Material section.

Radiosynthesis of [^{18}F]FHBT

The [^{18}F]KF solution was added to a sealed V-vial containing potassium carbonate (3.5 mg) and kryptofix 2.2.2 (15 mg). Water was removed by azeotropic drying with acetonitrile (3 × 0.35 ml) under He at 95 °C. The vial was heated for an additional 3 min under He. To this, anhydrous fluoride-kryptofix complex was added a solution

of the tosylate **7** (3–4 mg) in dry DMSO (0.6 ml). The reaction mixture was heated for 15 min at 160 °C. After cooling to room temperature, the crude product was diluted with water (10 ml), passed through 2× Sep-Pak cartridges (C_{18} plus) to remove kryptofix 2.2.2. and unreacted fluoride. The Sep-Pak was eluted with MeOH (2 ml). The effluent was acidified with 1 M HCl (0.5 ml), and the mixture was heated for 15 min at 100 °C. The vial was cooled to room temperature, neutralized with 1 M NaOH (0.5 ml), and diluted with water (2 ml). The crude product was purified by a semipreparative reverse phase HPLC system (column, Phenomenex, Gemini, Hesperia, CA, C18, 5 µm, 10 × 250 mm) with solvent A (water) and solvent B (acetonitrile) using a linear gradient from 95/5 (A/B) to 5/95 (A/B) over 30 min at a flow rate of 3 ml/min. A radioactive fraction with a retention time of 17.8 min was collected. Confirmation of the identity of [18F]FHBT was performed with authentic FHBT on an analytical HPLC system (column, Gemini C18, 250 × 4.6 mm) using the linear gradient from 95/5 (A/B) to 5/95 (A/B) over 20 min at a flow rate of 1.5 ml/min.

Cell Uptake Studies

The HSV1-sr39tk (+) MDA-MB-231 breast cancer cells were kindly provided by the laboratory of Dr. Ramasamy Paulmurugan (Stanford University, CA, USA). The cell uptake studies were performed according to previous literature [21, 22]. HSV1-sr39tk-positive or HSV1-sr39tk-negative MDA-MB-231 cells (from American Type Tissue Collection, ATCC) were cultured in high-glucose Dulbecco's modified Eagle's medium and supplemented with 10 % fetal bovine serum and 1 % penicillin/streptomycin solution. HSV1-sr39tk (+) cells were maintained in puromycin (100 ng/ml). The cells were seeded in 12 well tissue culture plates at a concentration of 1.0×10^5 cells per well in 1.0 ml of medium and were grown to 50–60 % confluence. After 24 h, 0.25 µCi of [3H]2-amino-9-[4-hydroxy-3-(hydroxymethyl)butyl]-1H-purin-6(9H)-one ([3H]penciclovir ([3H]PCV)) or 2.5 µCi of [18F]FHBT was added in each well and incubated at 37 °C for the appropriate times. Cells were then washed twice with 1× phosphate-buffered saline and lysed in RIPA buffer containing a protease inhibitor cocktail (Thermo Fisher Scientific, Waltham, MA). CytoScint scintillation fluid (MP Bio, Burlingame, CA) was added to the lysate of [3H]PCV-incubated cells, prior to counting by a scintillation counter (Beckman Coulter, Brea, CA). The counts associated with 100 µl of the lysate of [18F]FHBT-incubated cells were determined using a γ-counter. The protein concentrations in the lysates were determined using a bicinchoninic acid assay (BCA assay) (Thermo Fisher Scientific, Waltham, MA). All samples were compared with total activity references, and the percentage uptake per microgram of protein was calculated.

Small-Animal PET Studies

All animal procedures were performed in accordance with approved protocols by the Stanford University Administrative Panel on Laboratory Animal Care (APLAC). Tail vein catheters (12 cm polyurethane tubing and 27 g butterfly needle) (SAI Infusion, Lake Villa, IL) were inserted into the tail vein of 9 weeks old female BALB/c mice ($n = 4$ for [18F]FHBT and $n = 3$ for [18F]FHBG), and the catheter was held in place using Vet Bond tissue glue (3 M, Maplewood, MN). PET imaging was performed on a Siemens Inveon PET/CT scanner (Siemens Healthcare, Erlangen, Germany) (matrix size, 128 × 128 × 159; CT attenuation-corrected) after a bolus intravenous injection of [18F]FHBT or [18F]FHBG (7.4 MBq) into the mice. Dynamic scans were acquired in list mode for 60 mins. The acquired data were then sorted into 0.5-mm sinogram bins and 20 time frames for image reconstruction (5 × 15 s, 4 × 60 s, and 11 × 300 s), which was done by iterative reconstruction methods with the following parameters: 3D ordered-subset expectation maximization (3D-OSEM) followed by fast maximum *a posteriori* (fastMAP) reconstruction; MAPOSEM iterations, 2; MAP subsets, 16; and MAP iterations, 18. Regions-of-interest (ROIs) were drawn over the brain using the IRW software (Inveon Research Workplace, Siemens, Germany). All analyses were carried out using mean %ID/g.

Statistical Analysis

Statistical significance was determined at $P < 0.05$ using the one-way analysis of variance (ANOVA) for comparison of more than two means, followed by *post hoc* tests using Turkey's correction for the cell uptake experiments and the time-activity curves (TACs) of [18F]FHBT in the PET studies.

CNS PET MPO Score Calculation

Clog*P* and topological polar surface area (TPSA) were calculated using ChemBioDraw Ultra (version 13.0; PerkinElmer, Waltham, MA). Clog*D* and p*K*a were calculated using a SPARK online calculator. The central nervous system multiparameter PET optimization (CNS PET MPO) score calculation was performed as previously reported in the literature [23].

In Silico Predictions of Physicochemical and Biological Properties

The physicochemical and biopharmaceutical profiles of the investigated compounds were predicted with the ADMET Predictor software tool (version 8.5; Simulations Plus, Lancaster, CA) [24]. ADMET is short for absorption, distribution, metabolism, elimination, and toxicity. The

ADMET Predictor module contains different types of models (*e.g.*, p*K*a, partition, and transporters models, solubility models, permeability models, pharmacokinetic models, metabolism models, toxicity models, *etc.*) for its physicochemical and biological predictions. The ADMET Predictor software was designed using artificial neural network ensemble models trained with well-defined drugs and chosen for its high prediction accuracy. We used ADMET Predictor software to both qualify and quantify the likelihood of agents penetrating the BBB. ADMET Predictor's S+Pgp substrate model was used to predict the likelihood of P-glycoprotein (P-gp) efflux.

Results

Chemistry and Radiochemistry

The synthesis of FHBT was accomplished according to the pathway illustrated in Scheme 1. The 6-chloro-2-(phenylthio)-9H-purine (**1**) was synthesized as the starting material according to the methods described in the literature [20]. Compound **1** was reacted with 5-(2-Bromoethyl)-2,2-dimethyl-1,3-dioxane under a basic condition to give a mixture of the desired product 9-isomer purine (**2**) and undesired 7-isomer purine (**3**) in 48 and 9 % yield, respectively. Compounds **2** and **3** were successfully isolated by silica gel chromatography using $CHCl_3$/MeOH/EtOAc (20:1:1). The structure of each compound was identified by ^{1}H and ^{13}C-NMR as well as ESI mass spectrometry. Hydrolysis of compound **2** with aqueous hydrochloric acid, followed by neutralization afforded the deprotected diol compound **4** in 55 % yield. One hydroxy group of compound **4** was protected with monomethoxytrityl by the reaction of monomethoxytrityl chloride using DMAP and TEA under reflux, which gave monoprotected form compound **5** in 29 % yield. Compound **5** was reacted with *p*-tosyl chloride, affording precursor tosylate compound **6** in 43 % yield. Fluorination of compound **6** with 1 M TBAF in THF gave authentic FHBT in 87 % yield. The tosylate compound **6** was reacted with [^{18}F]KF using Kryptofix2.2.2 followed by deprotection to produce [^{18}F]FHBT in 10 % yield (decay corrected) as shown in Scheme 2. The yield of purified [^{18}F]FHBT was confirmed by analytical HPLC using the non-radioactive reference FHBT (Fig. S1).

Cellular Uptake Studies Using [^{3}H]PCV

To examine the interaction of HBT and FHBT with HSV1-TK, inhibitory experiments of these compounds against

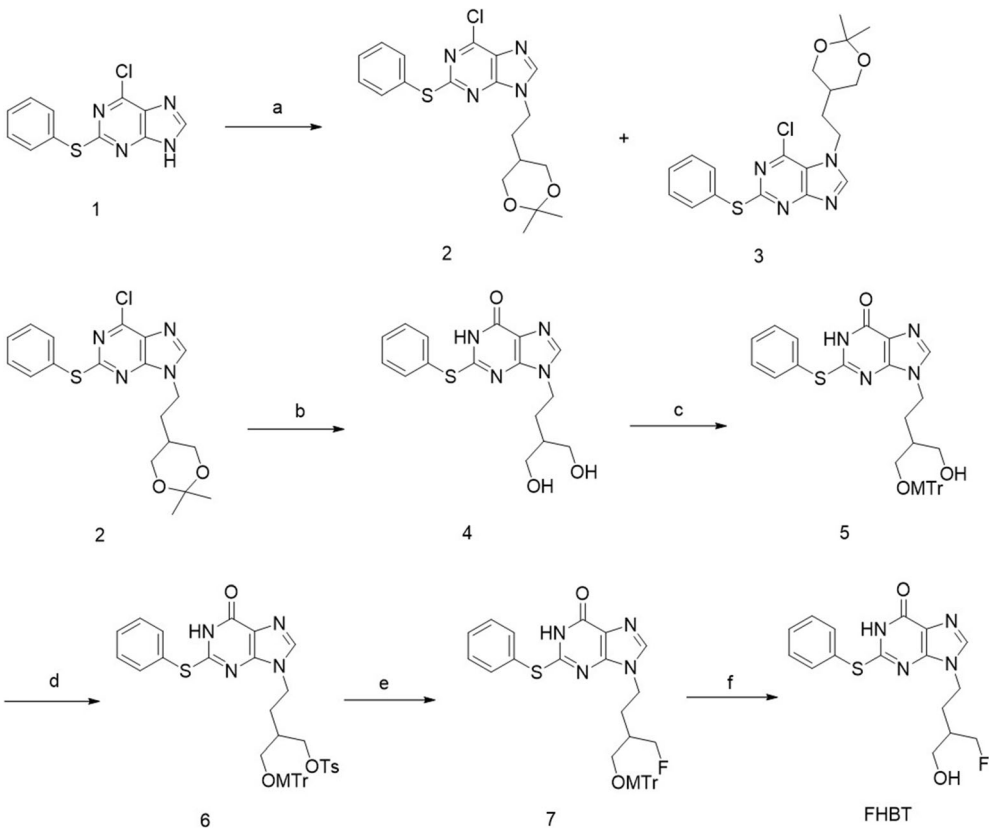

Scheme 1 Reagents and conditions: **a** 5-(2-bromoethyl)-2,2-dimethyl-1,3-dioxane, K_2CO_3, and DMF; **b** (1) HCl and THF and (2) NaOH; **c** 4-methoxytriphenylmethyl chloride, DMAP, TEA, and pyridine; **d** TsCl and pyridine; **e** TBAF and THF; and (f) HCl, MeOH.

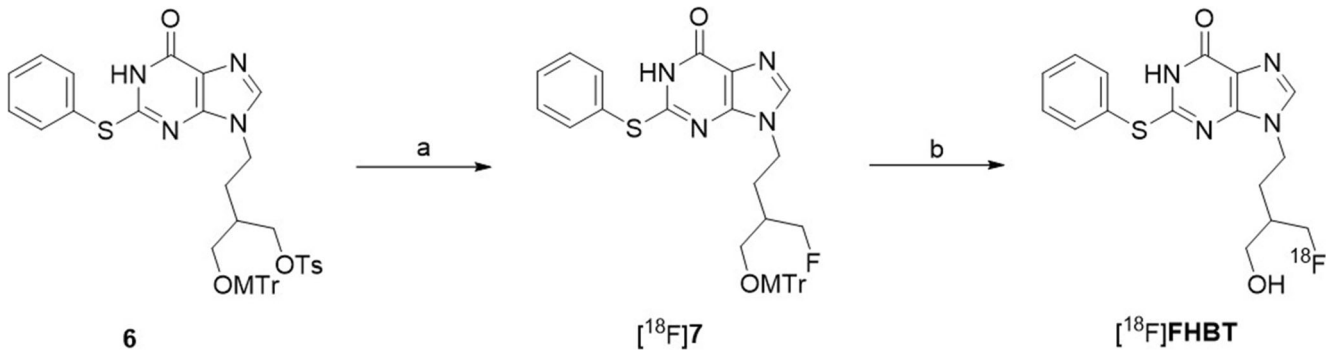

Scheme 2 Reagents and conditions: **a** K[^{18}F], Kryptofix 2.2.2, and CH_3CN; **b** HCl and MeOH.

radioactivity uptake of [^{3}H]PCV into HSV1-sr39tk-positive or HSV1-sr39tk-negative MDA-MB-231 cells were performed. Each cell line was incubated with [^{3}H]PCV in the absence or presence of compounds (0.01, 0.1, or 1 mM) for 30 min. We confirmed that [^{3}H]PCV showed high accumulation in the HSV1-sr39tk (+) cells (46.4 ± 2.52%uptake/mg protein), which is 35.1-fold higher than that of HSV1-sr39tk (−) cells (Fig. 2). In the presence of the well-known HSV1-TK and HSV1-sr39TK substrate 2-amino-9-(1,3-dihydroxypropan-2-yloxymethyl)-3H-purin-6-one (ganciclovir (GCV)) [25] at the concentrations of 0.01 and 0.1 mM, no significant decrease in the uptake of [^{3}H]PCV in HSV1-sr39tk (+) cells occurred ($P > 0.979$). Only the 1-mM concentration of GCV significantly blocked the uptake of [^{3}H]PCV by 86 %, as shown in Fig. 2a ($P < 0.001$). Although 0.01 mM of HBT led to a no marked reduction in the uptake of [^{3}H]PCV in HSV1-sr39tk (+) cells ($P = 0.12$), blockade with HBT at 0.1 and 1 mM significantly reduced the uptake by 53 and 94 % ($P < 0.001$), respectively. In addition, the uptake of [^{3}H]PCV in HSV1-sr39tk (+) cells was significant inhibited by 69 and 93 % ($P < 0.001$) in the presence of 0.1 and 1.0 mM FHBT, respectively. None of

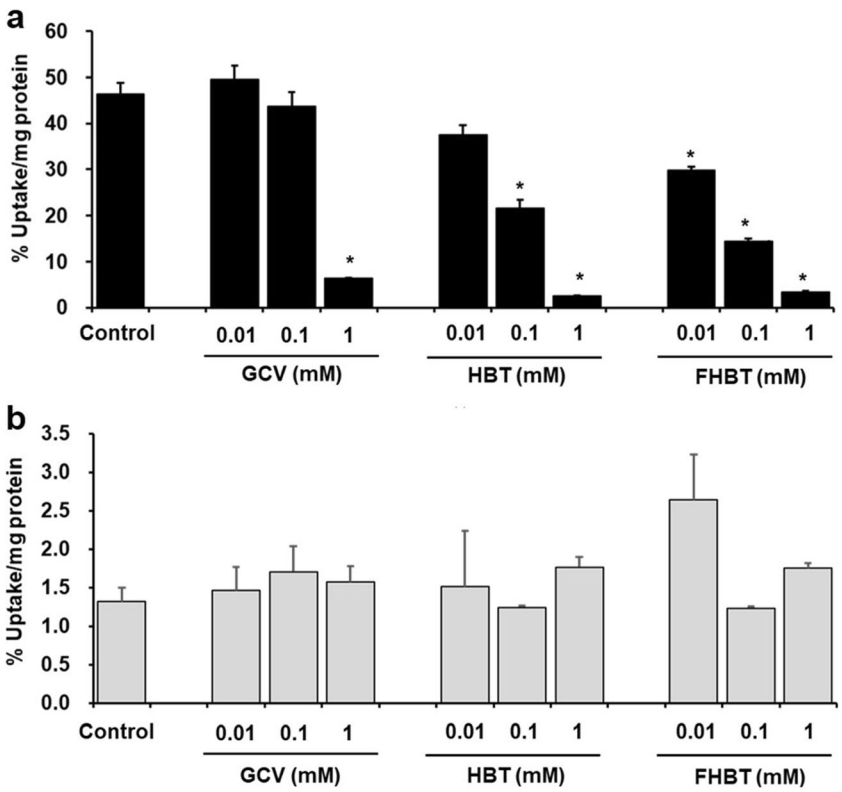

Fig. 2. Uptake of ^{3}H-PCV in HSV1-sr39tk-positive (**a**) or HSV1-sr39tknegative (**b**) MDA-MB-231 cells in the presence and absence of GCV, HBT, or FHBT at the indicated concentrations 30 min post-incubation. *$P < 0.001$ *versus* the control group (ANOVA, Tukey *t* test). Counts were normalized to %uptake/mg protein.

these three compounds showed significant blocking effects to the uptake of [3H]PCV in HSV1-sr39tk (−) cells ($P > 0.366$) (Fig. 2b).

Cellular Uptake Studies of [18F]FHBT

Next, we compared cellular uptake of [18F]FHBT and [3H]PCV at various incubation times (30, 60, 120, 180, and 240 min). As shown in Fig. 3a, [18F]FHBT showed time-dependent increase and high radioactivity uptake in HSV1-sr39tk (+) cells, with a plateau at 180 min (60.38 ± 5.66 % uptake/mg protein). The uptake of [18F]FHBT in HSV1-sr39tk (+) cells was drastically reduced in the presence of 1 mM of the anti-viral GCV compound (5.11 ± 0.37, 10.23 ± 2.79, 5.09 ± 0.51, and 11.41 ± 1.36 % uptake/mg protein at 30, 60, 120, 180, and 240 min, respectively), which is all significantly lower at each time point than the control groups ≥ 60 min ($P < 0.001$). [18F]FHBT uptakes in HSV1-sr39tk (−) cells were also significantly lower than those of HSV1-sr39tk (+) cells at each time point. The HSV1-tk-positive to HSV1-tk-negative cell ratio of [18F]FHBT uptake are 6.31-, 8.47-, 15.79-, 10.34-, and 6.91-fold higher at 30, 60, 120, 180, and 240 min, respectively. [3H]PCV uptake in HSV1-sr39tk (+) cells increased with time until 240 min and had higher uptake than those of [18F]FHBT at all time points (Fig. 3b). In the presence of GCV (1 mM), [3H]PCV uptake significantly decreased from 60 min, but the accumulation in HSV1-sr39tk (+) cells was still higher than those of [18F]FHBT. [3H]PCV showed relatively low uptake in HSV1-sr39tk (−) cells similar to [18F]FHBT at all time points. Both [18F]FHBT and [3H]PCV accumulations in HSV1-sr39tk (−) cells were not significantly affected by 1 mM of GCV.

PET Studies

Given [18F]FHBT is a selective substrate for HSV1-sr39TK, we next conducted PET studies of [18F]FHBT in normal mice ($n = 4$) to investigate the BBB permeability of this radioligand. PET studies of [18F]FHBG was also performed to determine its distribution within the normal brain ($n = 3$). Representative summed PET images of [18F]FHBT and [18F]FHBG from 5 to 60 min are shown in Fig. 4a, b, respectively. High uptake of [18F]FHBT in salivary glands and abdomen was visualized, whereas no significant brain uptake was observed. TACs of the whole-brain of mice intravenously injected with [18F]FHBT and [18F]FHBG at early and whole time frames are indicated in the Fig. 4c, d, respectively. Although there seems to be a small variation in the clearance rate between the two tracers until 12.75 min, their brain uptakes were not significant ($P > 0.855$) (Fig. 4c). [18F]FHBT and [18F]FHBG reached maximum level of %ID/g values in brain tissue at 0.623 and 0.375 min, respectively. Slower washout of [18F]FHBT was observed at the later time frames (17.75 − 57.75 min, $P > 0.207$), as shown in Fig. 4d, which might be due to higher lipophilicity of [18F]FHBT.

Discussion

There is a need for the development of BBB permeable PET probes for reporter gene imaging of HSV1-tk-expressing cells and its mutant variants. We designed [18F]FHBT

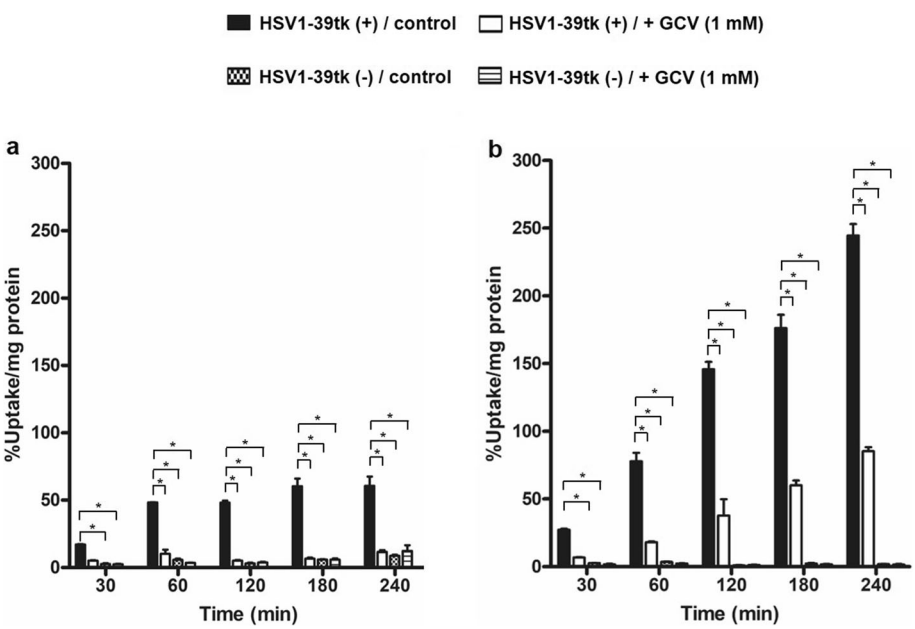

Fig. 3. Cellular uptake of [18F]FHBT (**a**) and [3H]PCV (**b**) in HSV1-sr39tk (+) or HSV1-39tk (–) MDA-MB-231 cells in the absence and presence of GCV (1 mM). Values represent mean ± standard error of the mean ($n = 3$). *$P < 0.001$ relative to HSV-1 39tk(+)/control groups at each time point. Counts were normalized to %uptake/mg protein.

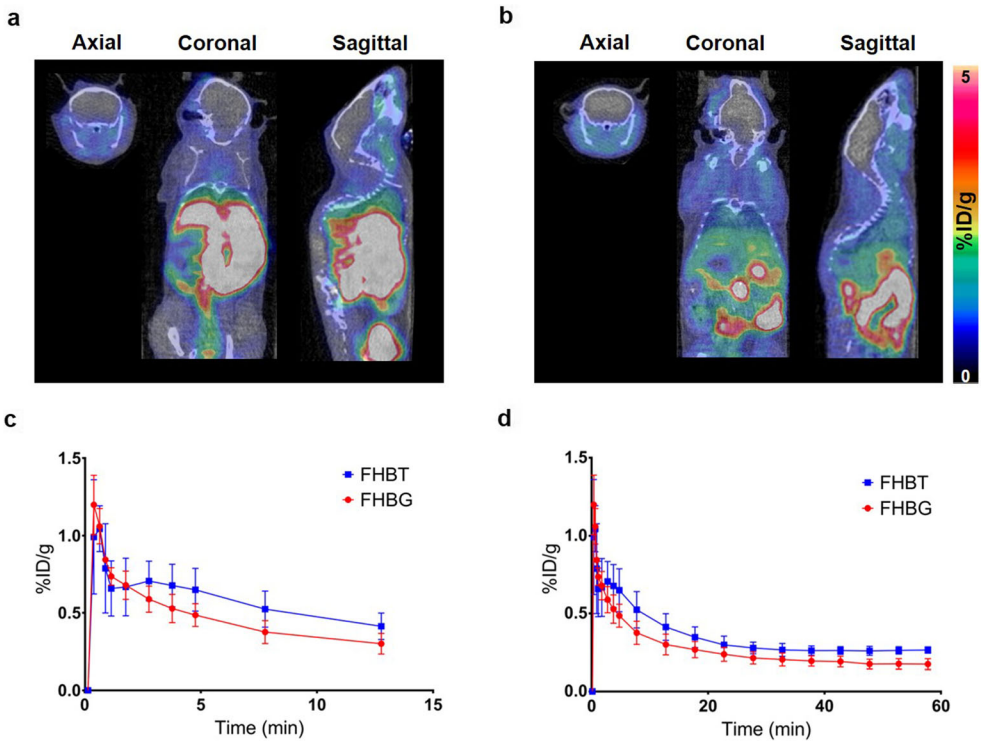

Fig. 4 Representative summed PET/CT images of [18F]FHBT (**a**) and [18F]FHBG (**b**) in BALB/c mice from 5 to 60 min after injection. Both of these tracers showed high uptake in salivary glands and abdomen but low uptake in the brain tissue. Time-activity curves of brain radioactivity after intravenous injection of [18F]FHBT ($n = 4$) or [18F]FHBG ($n = 3$) in mice at 0–20 min (**c**) and 0–60 min (**d**). Whole-brain uptake was expressed as a percentage of injected dose per gram of brain tissue (%ID/g).

(Clog$P$ = 1.98) as a new PET agent that combines structural features of [18F]FHBG and HBT [20], with high lipophilicity and high-affinity substrate properties for HSV1-TK enzymes. We have successfully synthesized the tosylate precursor **6** and [18F]FHBT using similar procedures previously reported [26]. We have also achieved the automated synthesis for [18F]FHBG [15] for clinical translation and plan to extend this to [18F]FHBT and its derivatives in the future. Cellular uptake studies using [3H]PCV indicated that HBT and FHBT competitively and strongly inhibit the internalization of [3H]PCV only in the HSV1-sr39tk (+) cells, and these compounds were expected to be a HSV1-sr39TK substrate or blocker. HBT and FHBT seem to possess stronger inhibitory activity of [3H]PCV uptake than that of GCV (Fig. 2). Although FHBT was demonstrated to inhibit [3H]PCV uptake into HSV1-sr39tk-expressing cells, it is unclear if this was due to HSV1-sr39TK inhibition or nucleoside transporter inhibition or both. [18F]FHBT exhibited high uptake in the HSV1-sr39tk (+) cells, while demonstrating low uptake in the HSV1-sr39tk (−) cells. MDA-MB-231 has various mammalian thymidine kinases [27]. Therefore, our results indicate that this radiotracer is a highly sensitive substrate for HSV1-sr39TK but a poor substrate for the other intracellular mammalian kinases. It is reported that *in vitro* accumulation of [18F]FHBG in HSV1-tk-expressing MDA-MB-468 cells was 9- to 13-fold higher than HSV1-tk (−) cells between 30 and 240 min post-tracer incubation [28]. In this study, the HSV1-sr39tk-positive to HSV1-sr39tk-negative cell ratio of [18F]FHBT uptake ranged from 6.31 to 15.79 at 30–240 min post-incubation, similar to that of [18F]FHBG. Compounds GCV, [18F]FHBG, and [18F]FHBT have structural similarity with guanosine, and GCV has been suggested to be transported by nucleoside transporters [3]. Similarly, [18F]FHBT may be internalized into cells *via* nucleoside transporters and trapped only in HSV1-sr39tk (+) cells. However, [18F]FHBT showed lower uptake than that of [3H]PCV in HSV1-sr39tk (+) cells at all time points (Fig. 3). Previously, we reported that [18F]FHBG and [3H]PCV showed similar uptake levels in C6 glioma cells stably transfected with mutant HSV1-sr39tk at 120 min post-tracer incubation [29]. Although the current study used different cell lines than previously reported [29], it is possible that introduction of a 2-phenylthiol group reduced uptake efficiency of [18F]FHBT *via* nucleoside transporters, phosphorylation rate of the 3′-hydroxymethyl group, or binding affinity to HSV1-TK as compared with [3H]PCV. Nevertheless, the use of [18F]FHBT as a reporter probe for PET imaging of HSV1-tk and its variant reporter genes is attractive because of its high specificity for HSV1-sr39TK and low background uptake in negative control cells.

The screening methods of BBB permeable PET probes with normal rodents have already been widely used for other brain imaging probes such as amyloid targeting PET probes

[30]. Therefore, we performed pilot PET studies of [^{18}F]FHBT in normal mice in this work. TACs from the brains of mice on the PET images (Fig. 4) suggested that [^{18}F]FHBT has no significant superiority as a PET probe targeting the reporter genes in the brain as compared with [^{18}F]FHBG. Despite having a moderate lipophilicity and a molecular weight under 400 Da, [^{18}F]FHBT demonstrated limited BBB penetration for *in vivo* imaging of brain tissue. Therefore, other factors should be considered for the development of successful BBB permeable PET agents for HSV1-tk reporter gene imaging.

It is reported that [^{18}F]FHBG showed good *in vivo* stability and at least 82 % of the intact tracer was detected in the urine sample 2 h after injection [31]. In this study, we found that both [^{18}F]FHBT and [^{18}F]FHBG reached maximum %ID/g values in the brain tissue within 1 min. Taken together, most of FHBT would remain intact at such an early time point. Recently, a central nervous system multiparameter PET optimization (CNS PET MPO) algorithm has been developed by a group from Pfizer for prediction of the required physicochemical properties of clinically useful CNS PET agents [23, 32]. They used a set of six parameters, including Clog*D* (calculated distribution coefficient at pH = 7.4), TPSA, topological polar surface area, HBD (number of hydrogen bond donors), and p*K*a (ionization constant of the most basic center) as important factors for CNS PET agents. In their algorithm, desirable ranges were set as Clog$P \leq 2.8$, Clog$D \leq 1.7$, MW ≤ 305.3, $44.8 <$ TPSA ≤ 63.3, HBD ≤ 1, and p$Ka \leq 7.2$. The scores of each parameter can be calculated ranging from 0.0 to 1.0. The most desirable and least desirable inflection points were set as 1.0 and 0.0, respectively. A linear function was used to determine the desirability scores between the inflection points [23, 32]. Most of the successfully translated CNS PET tracers in the Pfizer group's CNS PET ligand database had CNS PET MPO scores > 3 [23]. The physicochemical properties of FHBT were calculated as follows: Clog$P = 1.94$, Clog$D = 4.19$, TPSA = 77.29, MW = 348.4 Da, HBD = 2, and p$Ka = 7.57$. Using these parameters, the CNS PET MPO score of FHBT was calculated as follows: 1.00 for Clog*P*, 0.00 for Clog*D*, 0.389 for TPSA, 0.00 for MW, 0.00 for HBD, and 0.84 for p*K*a, giving a total CNS PET MPO score of 2.2. To increase the score to be above three, new FHBT derivatives should be developed in future research with further reduction in TPSA, MW, and HBD that could improve the initial brain uptake and rapid clearance from off-target regions.

In addition, there may be other reasons why [^{18}F]FHBT showed poor brain uptake. For example, FHBT may be a substrate for the P-glycoprotein efflux pump. Accordingly, we looked to see if FHBT is a potential substrate for the P-glycoprotein pump in the brain using the ADMET Predictor software (Simulations Plus, Lancaster, CA) [24]. Results from the *in silico* analysis showed that there was a predicted 62 % chance that FHBT would be a substrate for the P-glycoprotein efflux transporters at the BBB. Therefore, one reason that ^{18}F-FHBT exhibited low brain uptake may be due to efflux by the P-glycoprotein pump. Future efforts in developing BBB-permeable PET tracers for HSV1-tk and its mutants using the chemical scaffold of FHBT are thus warranted.

Conclusion

We have developed [^{18}F]FHBT as a new lipophilic PET radioligand for HSV1-sr39tk reporter gene imaging in brain tissue. The [^{18}F]FHBT tracer showed high specific uptake in HSV1-sr39tk expressing cells *in vitro*. Although our PET study demonstrated that [^{18}F]FHBT showed similar BBB permeability as [^{18}F]FHBG in normal mice, the FHBT scaffold can be used for future development of novel tracers for imaging gene expression of HSV1-tk and its variants in the living brain.

Acknowledgments. We thank the Radiochemistry Facility at Stanford University for ^{18}F-production. We would also like to thank Dr. Timothy Doyle at the Stanford Center for *In Vivo* Imaging (SCI^3) for his technical assistance. Additionally, we extend our thanks to Dr. Michael B. Bolger and John A. DiBella at Simulations Plus, Inc. for lending us access to the ADMET Predictor software tool.

Funding Information. Financial support was provided by the Ben and Catherine Ivy Foundation (S.S.G.). This work was also supported in part by Grants-in-Aid for Scientific Research (Fund for the Promotion of Joint International Research) and the Mochida Memorial Foundation for Medical and Pharmaceutical Research (T.F.).

Compliance with Ethical Standards

Conflict of Interest

The authors declare that they have no conflict of interest.

References

1. Li M, Wang Y, Liu M, Lan X (2018) Multimodality reporter gene imaging: construction strategies and application. Theranostics 8:2954–2973
2. Haywood T, Beinat C, Gowrishankar G, Patel CB, Alam IS, Murty S, Gambhir SS (2019) Positron emission tomography reporter gene strategy for use in the central nervous system. Proc Natl Acad Sci U S A 116:11402–11407
3. Min JJ, Gambhir SS (2008) Molecular imaging of PET reporter gene expression. Handb Exp Pharmacol:277–303
4. Brader P, Serganova I, Blasberg RG (2013) Noninvasive molecular imaging using reporter genes. J Nucl Med 54:167–172
5. Yaghoubi SS, Campbell DO, Radu CG, Czernin J (2012) Positron emission tomography reporter genes and reporter probes: gene and cell therapy applications. Theranostics 2:374–391
6. Yaghoubi SS, Barrio JR, Namavari M, Satyamurthy N, Phelps ME, Herschman HR, Gambhir SS (2005) Imaging progress of herpes simplex virus type 1 thymidine kinase suicide gene therapy in living subjects with positron emission tomography. Cancer Gene Ther 12:329–339
7. Alauddin MM, Shahinian A, Park R, Tohme M, Fissekis JD, Conti PS (2007) In vivo evaluation of 2′-deoxy-2′-[^{18}F]fluoro-5-iodo-1-beta-D-arabinofuranosyluracil ([^{18}F]FIAU) and 2′-deoxy-2′-[^{18}F]fluoro-5-ethyl-1-beta-D-arabinofuranosyluracil ([^{18}F]FEAU) as markers for suicide gene expression. Eur J Nucl Med Mol Imaging 34:822–829

8. Miyagawa T, Gogiberidze G, Serganova I, Cai S, Balatoni JA, Thaler HT, Ageyeva L, Pillarsetty N, Finn RD, Blasberg RG (2008) Imaging of HSV-tk reporter gene expression: comparison between [18F]FEAU, [18F]FFEAU, and other imaging probes. J Nucl Med 49:637–648
9. Brust P, Haubner R, Friedrich A, Scheunemann M, Anton M, Koufaki ON, Hauses M, Noll S, Noll B, Haberkorn U, Schackert G, Schackert HK, Avril N, Johannsen B (2001) Comparison of [18F]FHPG and [124/125I]FIAU for imaging herpes simplex virus type 1 thymidine kinase gene expression. Eur J Nucl Med 28:721–729
10. Alauddin MM, Conti PS (1998) Synthesis and preliminary evaluation of 9-(4-[^{18}F]-fluoro-3-hydroxymethylbutyl)guanine ([^{18}F]FHBG): a new potential imaging agent for viral infection and gene therapy using PET. Nucl Med Biol 25:175–180
11. Penuelas I, Haberkorn U, Yaghoubi S, Gambhir SS (2005) Gene therapy imaging in patients for oncological applications. Eur J Nucl Med Mol Imaging 32(Suppl 2):S384–S403
12. Yaghoubi SS, Jensen MC, Satyamurthy N, Budhiraja S, Paik D, Czernin J, Gambhir SS (2009) Noninvasive detection of therapeutic cytolytic T cells with 18F-FHBG PET in a patient with glioma. Nat Clin Pract Oncol 6:53–58
13. Keu KV, Witney TH, Yaghoubi S et al (2017) Reporter gene imaging of targeted T cell immunotherapy in recurrent glioma. Sci Transl Med 9:eaag2196
14. Black ME, Newcomb TG, Wilson HM, Loeb LA (1996) Creation of drug-specific herpes simplex virus type 1 thymidine kinase mutants for gene therapy. Proc Natl Acad Sci U S A 93:3525–3529
15. Yaghoubi SS, Gambhir SS (2007) PET imaging of herpes simplex virus type 1 thymidine kinase (HSV1-tk) or mutant HSV1-sr39tk reporter gene expression in mice and humans using [18F]FHBG. Nat Protoc 1:3069–3075
16. Martinez-Quintanilla J, Bhere D, Heidari P, He D, Mahmood U, Shah K (2013) Therapeutic efficacy and fate of bimodal engineered stem cells in malignant brain tumors. Stem Cells 31:1706–1714
17. Salabert AS, Vaysse L, Beaurain M et al (2017) Imaging grafted cells with [18F]FHBG using an optimized HSV1-TK mammalian expression vector in a brain injury rodent model. PloS One 12
18. Cunningham VJ, Parker CA, Rabiner EA, Gee AD, Gunn RN (2005) PET studies in drug development: methodological considerations. Drug Discov Today Technol 2:311–315
19. Pajouhesh H, Lenz GR (2005) Medicinal chemical properties of successful central nervous system drugs. NeuroRx 2:541–553
20. Manikowski A, Verri A, Lossani A, Gebhardt BM, Gambino J, Focher F, Spadari S, Wright GE (2005) Inhibition of herpes simplex virus thymidine kinases by 2-phenylamino-6-oxopurines and related compounds: structure-activity relationships and antiherpetic activity in vivo. J Med Chem 48:3919–3929
21. Sekar TV, Paulmurugan R (2013) ^{3}H-Penciclovir (^{3}H-PCV) uptake assay. Bio-protocol 3
22. Sekar TV, Foygel K, Ilovich O, Paulmurugan R (2014) Noninvasive theranostic imaging of HSV1-sr39TK-NTR/GCV-CB1954 dual-prodrug therapy in metastatic lung lesions of MDA-MB-231 triple negative breast cancer in mice. Theranostics 4:460–474
23. Zhang L, Villalobos A, Beck EM, Bocan T, Chappie TA, Chen L, Grimwood S, Heck SD, Helal CJ, Hou X, Humphrey JM, Lu J, Skaddan MB, McCarthy TJ, Verhoest PR, Wager TT, Zasadny K (2013) Design and selection parameters to accelerate the discovery of novel central nervous system positron emission tomography (PET) ligands and their application in the development of a novel phosphodiesterase 2A PET ligand. J Med Chem 56:4568–4579
24. ADMET Predictor™ [computer program], Simulations Plus, Inc., Lancaster, California, USA
25. Field AK, Davies ME, DeWitt C, Perry HC, Liou R, Germershausen J, Karkas JD, Ashton WT, Johnston DB, Tolman RL (1983) 9-([2-hydroxy-1-(hydroxymethyl)ethoxy]methyl)guanine: a selective inhibitor of herpes group virus replication. Proc Natl Acad Sci U S A 80:4139–4143
26. Zheng QH, Wang JQ, Liu X, Fei X, Mock BH, Glick-Wilson BE, Sullivan ML, Raikwar SP, Gardner TA, Kao C, Hutchins GD (2004) An improved Total synthesis of PET HSV-tk gene reporter probe 9-(4-[^{18}F]Fluoro-3-hydroxymethylbutyl)guanine ([^{18}F]FHBG). Synth Commun 34:689–704
27. RNA-seq of 934 human cancer cell lines from the Cancer Cell Line Encyclopedia. EMBL-EBI Expression Atlas
28. Alauddin MM, Shahinian A, Gordon EM, Conti PS (2004) Direct comparison of radiolabeled probes FMAU, FHBG, and FHPG as PET imaging agents for HSV1-tk expression in a human breast cancer model. Mol Imaging 3:76–84
29. Min JJ, Iyer M, Gambhir SS (2003) Comparison of [^{18}F]FHBG and [^{14}C]FIAU for imaging of HSV1-tk reporter gene expression: adenoviral infection vs stable transfection. Eur J Nucl Med Mol Imaging 30:1547–1560
30. Kung HF, Choi SR, Qu W, Zhang W, Skovronsky D (2010) 18F stilbenes and styrylpyridines for PET imaging of Aβ plaques in Alzheimer's disease: a miniperspective. J Med Chem 53:933–941
31. Yaghoubi S, Barrio JR, Dahlbom M, Iyer M, Namavari M, Satyamurthy N, Goldman R, Herschman HR, Phelps ME, Gambhir SS (2001) Human pharmacokinetic and dosimetry studies of [(18)F]FHBG: a reporter probe for imaging herpes simplex virus type-1 thymidine kinase reporter gene expression. J Nucl Med 42:1225–1234
32. Wager TT, Hou X, Verhoest PR, Villalobos A (2010) Moving beyond rules: the development of a central nervous system multiparameter optimization (CNS MPO) approach to enable alignment of druglike properties. ACS Chem Neurosci 1:435–449